# Peculiar Thermal Behavior of $UO_2$ Local Stucture

Damien Prieur,*[,†,‡,§] Enrica Epifano,[‖] Kathy Dardenne,[⊥] Joerg Rothe,[⊥] Christoph Hennig,[†,‡] Andreas C. Scheinost,[†,‡] Daniel R. Neuville,[#] and Philippe M. Martin[‖]

[†]Helmholtz Zentrum Dresden Rossendorf Institute of Resource Ecology, P.O. Box 10119, 01314 Dresden, Germany

[‡]Rossendorf Beamline (BM20 CRG), European Synchrotron Radiation Facility, 6 rue Jules Horowitz, BP 220, 38043 Grenoble, France

[§]European Commission, Joint Research Centre (JRC), Postfach 2340, 76125 Karlsruhe, Germany

[‖]CEA, Nuclear Energy Division, Research Department on Mining and Fuel Recycling Processes, SFMA, F 30207 Bagnols sur Cèze, France

[⊥]Karlsruhe Institute of Technology, Institute for Nuclear Waste Disposal (KIT INE), Hermann von Helmholtz Platz 1, D 76344 Eggenstein Leopoldshafen, Germany

[#]Géomatériaux, Institut de Physique du Globe de Paris CNRS, USPC 1 rue Jussieu, 75005 Paris, France

**ABSTRACT:** Most materials expand with temperature because of the anharmonicity of lattice vibration, and only a few shrink with increasing temperature. $UO_2$, whose thermal properties are of significant importance for the safe use of nuclear energy, was considered for a long time to belong to the first group. This view was challenged by recent *in situ* synchrotron X ray diffraction measurements, showing an unusual thermal decrease of the U−O distances. This thermal shrinkage was interpreted as a consequence of the splitting of the U−O distances due to a change in the U local order from *Fm*3*m* to *Pa*3. In contrast to these previous investigations and using an element specific synchrotron based spectroscopic method, we show here that the U sublattice remains locally of the fluorite type from 50 to 1265 K, and that the decrease of the first U−O bond lengths is associated with an increase of the disorder.

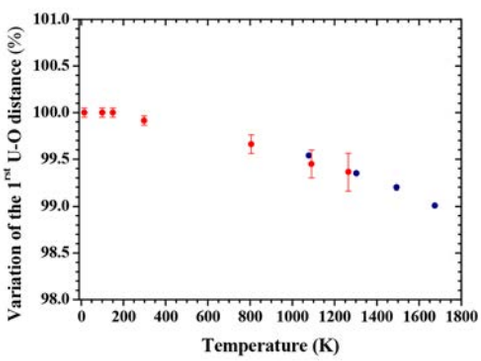


## INTRODUCTION

$UO_2$ is used in many countries as nuclear fuel for electrical power generation. Both its thermophysical and thermal properties at high temperatures are critical for the safe operation of nuclear reactors, as has been sadly demonstrated by the nuclear accidents of Chernobyl and Fukushima.[1]

Under ambient temperature, neutron diffraction has shown that $UO_2$ crystallizes in the fluorite structure ($CaF_2$):[2] the uranium cations form a face centered cubic lattice in which all the tetrahedral sites are occupied by oxygen anions.[3] In this *Fm*3*m* symmetry, each uranium atom is surrounded by eight oxygen atoms at 2.37 Å and 12 second neighbor uranium atoms at 3.87 Å. The thermal behavior of the $UO_2$ structure has been studied for decades notably by *in situ* X ray and neutron diffraction showing that the fluorite structure is maintained and that its lattice parameter expands.[4,5] Considering the *Fm*3*m* symmetry, one expects that the first U−O and U−U distances are proportional to the lattice parameter. At high temperature, $UO_2$ can no longer be described as a perfect fluorite structure with harmonic thermal vibrations of U and O on their respective sites. It was first erroneously attributed to relaxation of anions from their room temperature positions (1/4, 1/4, 1/4) to positions with slightly different coordinates (1/4+$\delta$, 1/4+$\delta$, 1/4+$\delta$).[6] The thermal evolution was later reproduced by including third cumulant coefficients which account for the anisotropic anharmonic thermal motion of the oxygen atoms remaining at the fluorite position (1/4, 1/4, 1/4).[7]

Several diffraction measurements at *circa* 1300 K showed a thermal increase of the U−O distances as well as of the unit cell.[6,8,9] In contrast, more recent synchrotron X ray diffraction measurements by Skinner et al.[10] contradict these observa tions. Indeed, the corresponding atomic pair distribution function (PDF) results indicate that the first U−O bond length contracts on heating up to the melting point (3147 ± 20 K[11]) whereas the intermetallic distance expands. It is assumed that the U−O contraction results from the existence of atomic disorder in the anion lattice. Subsequent neutron PDF results obtained by Desgranges et al.[12] also support the shortening of the U−O bonds, but a splitting of the O shell into two U−O distances was evident. Hence, these measurements showed that with the temperature the local order around U changes from *Fm*3*m* to *Pa*3.

From this short review, one can see that differences exist on both the local environment of $UO_2$ at high temperature and the thermal behavior of the U−O distances. Here, we use *in situ* X ray Absorption Spectroscopy (XAS) spectroscopy to

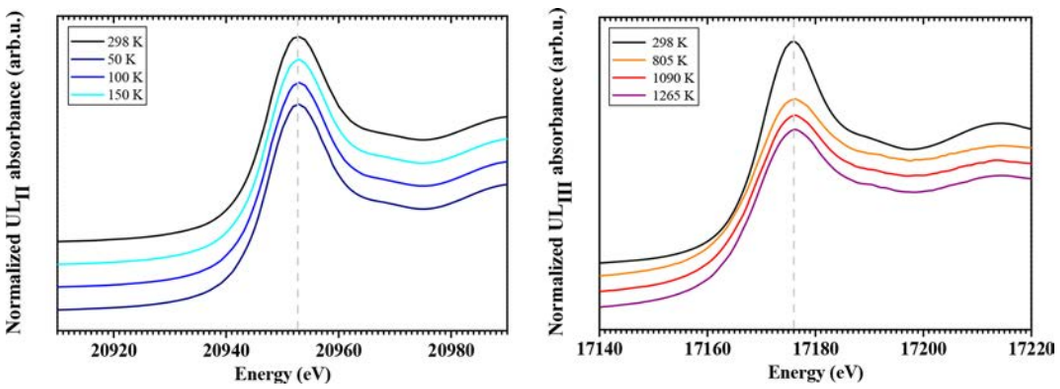


**Figure 1.** XANES spectra of stoichiometric $UO_{2.00}$. (Left) $UL_{II}$ XANES spectra of $UO_{2.00}$ at 50, 100, 150, and 298 K.[19] (Right) $UL_{III}$ XANES spectra of $UO_{2.00}$ at 298,[22] 805, 1090, and 1265 K. The dashed gray line indicates that all the spectra recorded in temperature are aligned on the $UO_{2.00}$ white line at room temperature.

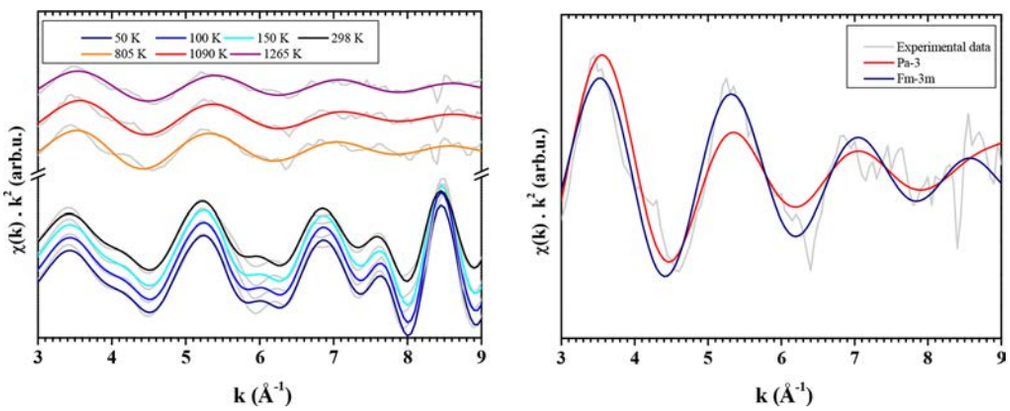


**Figure 2.** (Left) EXAFS spectra of stoichiometric $UO_{2.00}$. Fitted and experimental $k^2$ weighted EXAFS spectra of $UO_{2.00}$ collected at several temperatures. The experimental data are in light gray and the data fitted with the *Fm*3*m* space group are colored. Note that for the temperatures 50, 100, and 150 K, the EXAFS spectra were collected at the $UL_{II}$ edge. (Right) EXAFS spectra at 1265 K fitted using *Fm*3*m* (blue line) and *Pa*3 (red line) models.

tackle this discrepancy, by studying the evolution of the local structure around U in $UO_2$ as a function of temperature from 50 to 1300 K.

## EXPERIMENTAL DETAILS

*In situ* X ray Absorption Near Edge Spectroscopy (XANES) and Extended X ray Absorption Fine Structure (EXAFS) measurements were conducted at the ROBL beamline[13] (ESRF, Grenoble, France) and at the INE Beamline of the KIT synchrotron light source (Karlsruhe Institute of Technology, Karlsruhe, Germany).[14]

**XAS Data Acquisition.** The XAS spectra from 50 to 150 K were collected at ROBL at the U $L_{II}$ edge on $UO_2$ samples that have been previously sintered in Ar 4% $H_2$ at 2023 K during 4 h. Based on $UO_2$ thermodynamics,[15] these heating conditions ensure a stoichiometric oxide.[4] Note that U $L_{II}$ was measured instead of U $L_{III}$ as these measurements were coupled with other acquisitions performed at U $L_{II}$. The storage ring operating conditions were 6.0 GeV and 170−200 mA. Double crystal monochromator mounted with Si (111) crystals were used. Samples were held at 15, 100, and 150 K using a closed cycle helium cryostat. Data were collected in both transmission and fluorescence modes at the uranium $L_{II}$ (20 948 eV) edge. Energy calibration was achieved by measuring the K XANES spectrum of a Mo reference foil (20 000 eV) located between the second and third ionization chambers. Fluorescence signal was measured with a 13 element Ge solid state detector using a digital amplifier.

The XAS measurements from RT to 1300 K were recorded at INE at the U $L_{III}$ edge with a dedicated furnace on a fragment extracted from the same dense (98%) sintered $UO_{2.00}$ pellet used at ROBL. The furnace atmosphere was held constant in Ar 4% $H_2$ to maintain the stoichiometry.[4] Prior to measurement, the sample is mechanically fixed on a Pt/Ir (90/10) wire. This heating element is then inserted into a dedicated furnace which allows collection of *in situ* XAS data on radioactive samples in various atmospheres and up to 2000 K.[16] The storage ring operating conditions were 2.5 GeV and 100−160 mA. A Ge [422] double crystal monochromator coupled with collimating and focusing Rh coated mirrors was used. XAS spectra were collected at various temperatures in fluorescence mode at the U $L_{III}$ edge (17 166 eV) with a five element germanium solid state detector. Energy calibration was achieved by measuring the K XANES spectrum of a Y reference foil (17 038 eV) located between the second and third ionization chambers. The experimental data have been collected in Ar 4% $H_2$ at 298, 805, 1090, and 1265 K. During each of these successive temperature plateaus, 4 U $L_{III}$ EXAFS scans have been collected. Note that the Pt/Ir wire temperature was calibrated before the measurement.

**In Situ XAS.** A complete review of the heating wire can be find in Neuville et al.[16] The heating wire is a platinum or platinum alloy wire with a diameter between 1 and 2 mm, flattened in the middle with a hole with a diameter from 100 $\mu$m up to 1 mm. This hole corresponds to the hot spot. This heating system has low thermal inertia and it is possible to change the temperature between room temperature up to temperatures >1973 K in a few seconds. At temperature, the heating system is relatively stable and can stay at the selected temperature as long as needed during the experiments.

**XAS Data Analysis.** The XANES spectra have been normalized using linear functions for pre and post edge modeling. The white line maxima have been taken as the first zero crossing of the first

derivative. Pre edge removal, normalization, and self absorption correction were performed using the ATHENA software.[17]

The EXAFS oscillations, collected up to 14 $Å^{-1}$, were extracted from the raw absorption spectra with the ATHENA software[17] and Fourier transformed using a Hanning window over the $k^2$ range [3−9] $Å^{-1}$. Phases and amplitudes for the interatomic scattering paths were calculated with the *ab initio* code FEFF 8.40.[18] Both *Fm*3*m* and *Pa*3 symmetries have been used as structural models in the FEFF calculations to fit the EXAFS spectra. In the former space group, the first anion shell is composed of eight equidistant oxygen atoms, while in the latter the $UO_8$ polyhedron is a distorted oxygen cube with two longer and six shorter distances. According to the literature on actinides EXAFS data treatment,[19−21] the amplitude factor ($S_0^2$) was set at 0.90. The shift in the threshold energy ($\Delta E_0$) was varied as a global parameter.

## RESULTS AND DISCUSSION

Comparing the collected XANES spectra with a $UO_{2.00}$ reference measured at 298 K on both beamlines,[19,22] we observe that our investigated $UO_2$ remains stoichiometrically independently of the temperature (Figure 1). Any deviation from the stoichiometry of the compound would be identifiable from U $L_{II,III}$ XANES by a shift of the white line toward lower (i.e., reduction) or higher (i.e., oxidation) energy.[20,22−24] One should note that, contrary to the previously mentioned investigations on $UO_2$, this direct measurement of the U oxidation state ensures that the acquired data really refer to a stoichiometric compound.

While heating from 50 to 1265 K, no strong modification of the local environment can be observed in the experimental EXAFS spectra (Figure 2 (Left)). The main visual evolution is a damping of the EXAFS oscillations, especially at high $k$ values, due to the increase of the thermal vibration. For this reason, only the first U−O bond lengths have been fitted for each EXAFS spectrum.

Taking into account the findings of Skinner et al.[10] and Desgranges et al.,[12] each EXAFS spectrum has been fitted independently of the temperature using both *Fm*3*m* and *Pa*3 structural models. In the former, the first anion shell is composed of eight equidistant oxygen atoms ($r_{U-O}$ = *ca.* 2.37 Å) while in the latter the $UO_8$ polyhedron is a distorted oxygen cube with six shorter distances ($r_{U-O}$ = *ca.* 2.34 Å) and two longer ($r_{U-O}$ = *ca.* 2.56 Å).[12] Note that neither clustering of oxygen interstitials (i.e., Willis or cuboctahedral clusters) nor shorter U−O distances have been observed, the latter having already being reported in $UO_{2+x}$ phases.[25] For all temperatures, the best refinements are achieved using a *Fm*3*m* structural model. Even if the fit residuals value is rather good, the crystallographic parameters derived from the *Pa*3 symmetry are very far off from the values determined by Desgranges and seem not to be reasonable. As an example, the *Pa*3 EXAFS derived structural parameters of the $UO_2$ samples heated at 1275 K are given in Table 1 and the corresponding spectra are presented in the Figure 2 (Right). One can note that close values of the residual factors are obtained with both models. However, the fitted Debye−Waller factors are high (>0.025 $Å^2$) in the case of *Pa*3, and more importantly the distances do not converge toward the model values. On the contrary they diverge from reasonable values for a distorted $UO_8$ polyhedron. Contrary to the work of Desgranges et al.,[12] our experimental data indicate that the local *Fm*3*m* environment remains and no thermal transition occurs toward the lower *Pa*3 symmetry. The present results do not support a local change of space group with temperature. One of the reasons that could explain this discrepancy is a difference of stoichiometry of the studied compounds. Indeed, the $UO_{2+x}$ solid solution is known to have a large hyperstoichiometric domain for temperatures above 600 K. Moreover, several other phases with different crystal structures exist in the U−O phase diagram, depending on the temperature and the stoichiometry.[15] The latter is notably very sensitive to the oxygen partial pressure during the experimental treatment. In this study, the measurements were carried out in Ar 4%$H_2$ while the neutron diffraction data of Desgranges et al.[12] were collected using a container sealed under vacuum. In principle, that configuration should not lead to a reduction toward $UO_{2-x}$ or an (appreciable) oxidization from $UO_{2.00}$ to $UO_{2+x}$, but no experimental measurement of the stoichiometry was performed to confirm this assumption. On the contrary, here we used XANES, which is a direct, powerful and acknowledged technique,[19,22−24] to derive the uranium oxidation states and to ensure that $UO_{2.00}$ remains stoichiometric and that no $UO_{2+x}$ phase was formed during the thermal treatment.

**Table 1. Structural Parameters**[a]

| Structural parameters | *Fm*$\bar{3}$*m** | *Pa*$\bar{3}$* | | *Pa*$\bar{3}$[12] | |
|---|---|---|---|---|---|
| R (Å) | 2.343 (6) | 2.29 (1) | 2.73 (1) | 2.34 | 2.56 |
| N | 7.5 (1.2) | 6 | 2 | 6 | 2 |
| $\sigma^2$ ($Å^2$) | 0.017 (3) | 0.025 (5) | 0.025 (5) | | |
| $R_f$ ($\subseteq 10^{-3}$) | 8 | 12 | | | |

[a]The interatomic distances $R$, the coordination numbers $N$, and the Debye Waller factors $\sigma^2$ were derived from the EXAFS spectra at 1265 K using either a *Fm*3*m* or *Pa*3 structural model. For the *Pa*3 fitting, the coordination numbers were fixed to the theoretical values as otherwise no convergence was achieved. The uncertainties are the numbers in brackets. Our data (noted with a * in the table) are compared with those of Desgranges et al.[12]

The interatomic distances, the coordination numbers, and the Debye−Waller factors were then derived for each temperature by fitting all the EXAFS spectra with a *Fm*3*m* structure (Figure 3). From 50 to 298 K, no significant variation of the structural parameters has been noted. For these temperatures, the $UO_8$ polyhedron is composed of one uranium atom neighbored by 8.0 (5) oxygen anions at 2.358 (3) Å. While heating from 298 to 1265 K, significant variations of these crystallographic parameters are observed. There is a decrease of the first U−O bond length, which is quantitatively and qualitatively in good agreement with the neutron measurements of Skinner et al.[10] (Figure 3 (Top right)). Although within the error bar, the coordination seems to drop as well, which again would agree with Skinner et al.[10] who reported a value of 6.7 (5) at 3270 K. However, based on molecular dynamic simulation,[26] they also argue that the coordination number should essentially have a constant value of 8 up to the melting point and that, only then, is there a rearrangement toward $UO_{6.7(5)}$ polyhedron. Considering the error bar on our EXAFS derived coordination numbers, we can neither confirm nor exclude this proposed mechanism. We can only say that our results suggest that there is already below the melting point a rearrangement of the oxygen coordination shell around uranium, which indeed would be supported by the observed contraction of the first U−O distances. In addition, we observed an increase of the Debye−Waller factors, which corresponds to the parallel mean square relative displacement and parametrizes the variance of the distance distribution. In other terms, it accounts for the effects of structural and

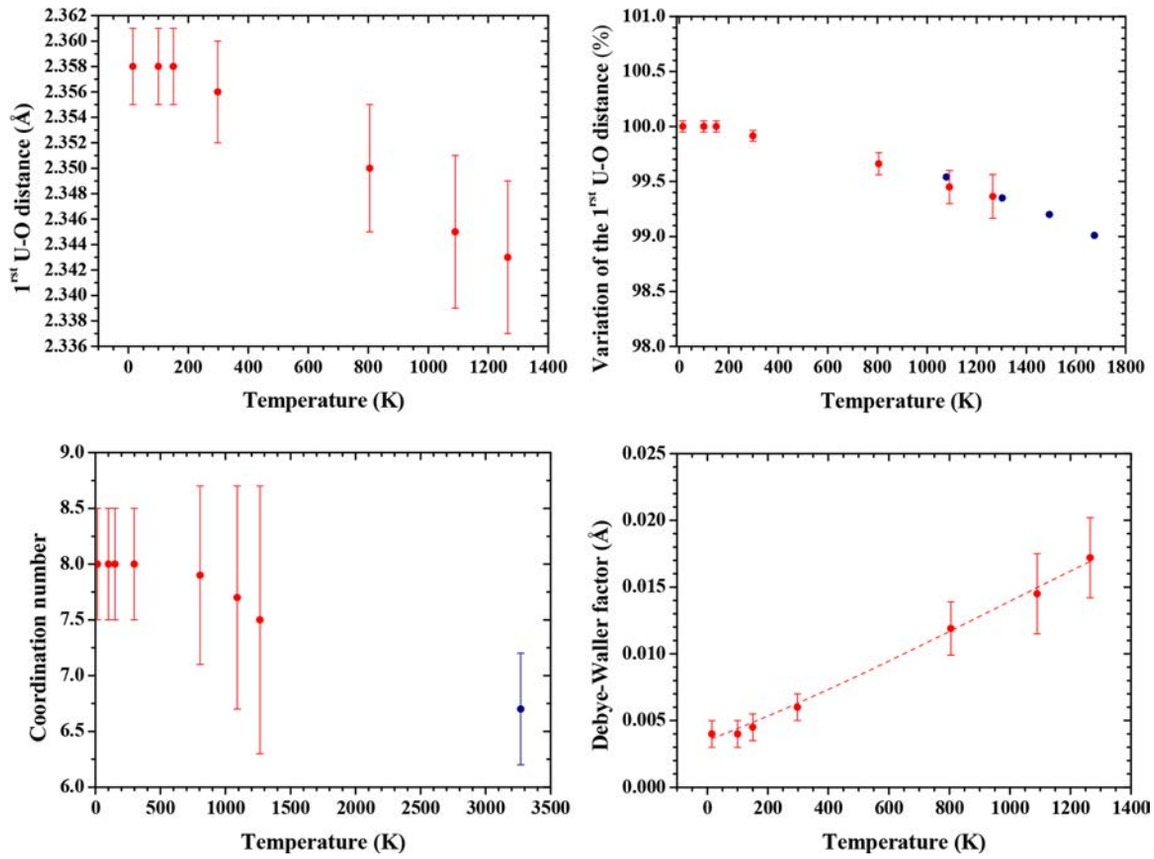


**Figure 3.** Temperature dependence of the EXAFS derived structural parameters of stoichiometric $UO_{2.00}$. (Top left) The first U−O fitted distances as a function of the temperature. (Top right) The first U−O fitted distances are normalized to the 15 K value and compared to the experimental data of Skinner et al.,[10] which are represented with blue circles. (Bottom left) The coordination numbers of the first O shell as a function of the temperature. (Bottom right) The Debye−Waller factors derived from the EXAFS analysis of the first U−O distances as a function of the temperature (red open circle). These have been fitted using the Einstein model (red straight line) and the calculated Einstein temperature is $\theta_E$ = 480 ± 20 K.

vibrational disorder. In our case, the observed increase of the Debye−Waller factor can mainly be attributed to the vibrational disorder, as the static contribution seldom exhibits temperature dependence.[27] This disorder is likely due to the displacement of the oxygen anions from their native sites. In that case, a monotonic increase with temperature is expected, as in our case for temperatures ranging from 600 to 1265 K.[28] Our experimental values were satisfactorily fitted using the Einstein model[29] and an Einstein temperature of 480 ± 20 K was found, which is slightly lower than previously reported values, i.e., 542 K[30] and 620 K.[31]

## CONCLUSION

As the majority of operating nuclear reactors are fueled with $UO_2$, demonstrating and quantifying the contraction of the local $UO_2$ structure with the temperature is an essential ingredient in assessing the safety relevant behavior of this material. Indeed, current calculation codes are only based on the expansion of the whole lattice, i.e., both interatomic distances and unit cell. These same theoretical models are used notably to predict the behavior of the fuel in normal and off conditions. However, our present results clearly show that one cannot assume that the anionic interatomic distances expand with the temperature. On the contrary, they contract, which means that the overall volume of the interstitial sites decreases. Consequently, our current understanding of the accommodation of fission products in the $UO_2$ structure needs deeper consideration to enable even better understanding of the operation safety of $UO_2$ nuclear fuel.

## AUTHOR INFORMATION


### Corresponding Author

*E mail: d.prieur@hzdr.de.

### ORCID

Damien Prieur: 0000 0001 5087 0133

Enrica Epifano: 0000 0001 5327 0491

Christoph Hennig: 0000 0001 6393 2778

Andreas C. Scheinost: 0000 0002 6608 5428


### Author Contributions

The manuscript was written through contributions of all authors. All authors have given approval to the final version of the manuscript.

### Notes

The authors declare no competing financial interest.

## ACKNOWLEDGMENTS


We acknowledge the KIT light source for provision of instruments at their beamlines and we would like to thank the Institute for Beam Physics and Technology (IBPT) for the operation of the storage ring, the Karlsruhe Research Accelerator (KARA). We are also thankful to the ESRF

synchrotron for provision of beamtime. We are entitled to both ROBL and INE teams for their help during the measurements.

## REFERENCES

(1) Konings, R. J. M.; Wiss, T.; Beneš, O. Predicting material release during a nuclear reactor accident; https://www.nature.com/articles/nmat4224 (accessed Apr 3, 2018).

(2) Willis, B. T. M. Neutron Diffraction Studies of the Actinide Oxides. I. Uranium Dioxide and Thorium Dioxide at Room Temperature. *Proc. R. Soc. London, Ser. A* **1963**, *274* (1356), 122−133.

(3) Willis, B. T. M. Positions of the Oxygen Atoms in UO2.13. *Nature* **1963**, *197* (4869), 755−756.

(4) Guéneau, C.; Chartier, A.; Van Brutzel, L. 2.02 Thermodynamic and Thermophysical Properties of the Actinide Oxides. In *Comprehensive Nuclear Materials*, Konings, R. J. M., Ed.; Elsevier: Oxford, 2012; pp 21−59.

(5) Guthrie, M.; Benmore, C. J.; Skinner, L. B.; Alderman, O. L. G.; Weber, J. K. R.; Parise, J. B.; Williamson, M. Thermal Expansion in UO2 Determined by High Energy X Ray Diffraction. *J. Nucl. Mater.* **2016**, *479*, 19−22.

(6) Willis, B. T. M. Structures of UO2, UO2+x AndU4O9 by Neutron Diffraction. *J. Phys. Radium* **1964**, *25* (5), 431−439.

(7) Willis, B. T. M.; Hazell, R. G. Re Analysis of Single Crystal Neutron Diffraction Data on UO2 Using Third Cumulants. *Acta Crystallogr., Sect. A: Cryst. Phys., Diffr., Theor. Gen. Crystallogr.* **1980**, *36* (4), 582−584.

(8) Albinati, A.; Cooper, M. J.; Rouse, K. D.; Thomas, M. W.; Willis, B. T. M. Temperature Dependence of the Atomic Thermal Displacements in UO2: A Test Case for the Rietveld Profile Refinement Procedure. *Acta Crystallogr., Sect. A: Cryst. Phys., Diffr., Theor. Gen. Crystallogr.* **1980**, *36* (2), 265−270.

(9) Ruello, P.; Desgranges, L.; Baldinozzi, G.; Calvarin, G.; Hansen, T.; Petot Ervas, G.; Petot, C. Heat Capacity Anomaly in UO2 in the Vicinity of 1300K: An Improved Description Based on High Resolution X Ray and Neutron Powder Diffraction Studies. *J. Phys. Chem. Solids* **2005**, *66* (5), 823−831.

(10) Skinner, L. B.; Benmore, C. J.; Weber, J. K. R.; Williamson, M. A.; Tamalonis, A.; Hebden, A.; Wiencek, T.; Alderman, O. L. G.; Guthrie, M.; Leibowitz, L.; et al. Molten Uranium Dioxide Structure and Dynamics. *Science* **2014**, *346* (6212), 984−987.

(11) Manara, D.; Ronchi, C.; Sheindlin, M.; Lewis, M.; Brykin, M. Melting of Stoichiometric and Hyperstoichiometric Uranium Dioxide. *J. Nucl. Mater.* **2005**, *342* (1), 148−163.

(12) Desgranges, L.; Ma, Y.; Garcia, P.; Baldinozzi, G.; Siméone, D.; Fischer, H. E. What Is the Actual Local Crystalline Structure of Uranium Dioxide, UO2? A New Perspective for the Most Used Nuclear Fuel. *Inorg. Chem.* **2017**, *56* (1), 321−326.

(13) Matz, W.; Schell, N.; Bernhard, G.; Prokert, F.; Reich, T.; Claußner, J.; Oehme, W.; Schlenk, R.; Dienel, S.; Funke, H.; et al. ROBL − a CRG Beamline for Radiochemistry and Materials Research at the ESRF. *J. Synchrotron Radiat.* **1999**, *6* (6), 1076−1085.

(14) Rothe, J.; Butorin, S.; Dardenne, K.; Denecke, M. A.; Kienzler, B.; Löble, M.; Metz, V.; Seibert, A.; Steppert, M.; Vitova, T.; et al. The INE Beamline for Actinide Science at ANKA. *Rev. Sci. Instrum.* **2012**, *83* (4), 043105.

(15) Guéneau, C.; Baichi, M.; Labroche, D.; Chatillon, C.; Sundman, B. Thermodynamic Assessment of the Uranium−Oxygen System. *J. Nucl. Mater.* **2002**, *304* (2), 161−175.

(16) Neuville, D. R.; Hennet, L.; Florian, P.; de Ligny, D. In Situ High Temperature Experiments. *Rev. Mineral. Geochem.* **2014**, *78* (1), 779−800.

(17) Ravel, B.; Newville, M. ATHENA, ARTEMIS, HEPHAESTUS: Data Analysis for X Ray Absorption Spectroscopy Using IFEFFIT. *J. Synchrotron Radiat.* **2005**, *12* (4), 537−541.

(18) Rehr, J. J.; Kas, J. J.; Vila, F. D.; Prange, M. P.; Jorissen, K. Parameter Free Calculations of X Ray Spectra with FEFF9. *Phys. Chem. Chem. Phys.* **2010**, *12* (21), 5503−5513.

(19) Prieur, D.; Martin, P. M.; Jankowiak, A.; Gavilan, E.; Scheinost, A. C.; Herlet, N.; Dehaudt, P.; Blanchart, P. Local Structure and Charge Distribution in Mixed Uranium Americium Oxides: Effects of Oxygen Potential and Am Content. *Inorg. Chem.* **2011**, *50* (24), 12437−12445.

(20) Prieur, D.; Lebreton, F.; Martin, P. M.; Caisso, M.; Butzbach, R.; Somers, J.; Delahaye, T. Comparative XRPD and XAS Study of the Impact of the Synthesis Process on the Electronic and Structural Environments of Uranium Americium Mixed Oxides. *J. Solid State Chem.* **2015**, *230*, 8−13.

(21) Prieur, D.; Martin, P.; Lebreton, F.; Delahaye, T.; Banerjee, D.; Scheinost, A. C.; Jankowiak, A. Accommodation of Multivalent Cations in Fluorite Type Solid Solutions: Case of Am Bearing UO2. *J. Nucl. Mater.* **2013**, *434* (1−3), 7−16.

(22) Martel, L.; Vigier, J. F.; Prieur, D.; Nourry, S.; Guiot, A.; Dardenne, K.; Boshoven, J.; Somers, J. Structural Investigation of Uranium Neptunium Mixed Oxides Using XRD, XANES, and O 17 MAS NMR. *J. Phys. Chem. C* **2014**, *118* (48), 27640−27647.

(23) Boehler, R.; Welland, M. J.; Prieur, D.; Cakir, P.; Vitova, T.; Pruessmann, T.; Pidchenko, I.; Hennig, C.; Gueneaud, C.; Konings, R. J. M.; et al. Recent Advances in the Study of the UO2 PuO2 Phase Diagram at High Temperatures. *J. Nucl. Mater.* **2014**, *448* (1−3), 330−339.

(24) Smith, A. L.; Martin, P.; Prieur, D.; Scheinost, A. C.; Raison, P. E.; Cheetharn, A. K.; Konings, R. J. M. Structural Properties and Charge Distribution of the Sodium Uranium, Neptunium, and Plutonium Ternary Oxides: A Combined X Ray Diffraction and XANES Study. *Inorg. Chem.* **2016**, *55* (4), 1569−1579.

(25) Conradson, S. D.; Manara, D.; Wastin, F.; Clark, D. L.; Lander, G. H.; Morales, L. A.; Rebizant, J.; Rondinella, V. V. Local Structure and Charge Distribution in the UO2−U4O9 System. *Inorg. Chem.* **2004**, *43* (22), 6922−6935.

(26) Yakub, E.; Ronchi, C.; Staicu, D. Molecular Dynamics Simulation of Premelting and Melting Phase Transitions in Stoichiometric Uranium Dioxide. *J. Chem. Phys.* **2007**, *127* (9), 094508.

(27) Fornasini, P.; Grisenti, R. On EXAFS Debye Waller Factor and Recent Advances. *J. Synchrotron Radiat.* **2015**, *22* (5), 1242−1257.

(28) Annamareddy, A.; Eapen, J. Disordering and Dynamic Self Organization in Stoichiometric UO2 at High Temperatures. *J. Nucl. Mater.* **2017**, *483*, 132−141.

(29) Sevillano, E.; Meuth, H.; Rehr, J. J. Extended X Ray Absorption Fine Structure Debye Waller Factors. I. Monatomic Crystals. *Phys. Rev. B: Condens. Matter Mater. Phys.* **1979**, *20* (12), 4908−4911.

(30) IAEA. Thermodynamic and Transport Properties of Uranium Dioxide and Related Phases.

(31) Dolling, G.; Cowley, R. A.; Woods, A. D. B. The Crystal Dynamics of Uranium Dioxide. *Can. J. Phys.* **1965**, *43* (8), 1397−1413.